Published in final edited form as:
Neurosci Lett. 2010 May 21; 475(3): 136–140. doi:10.1016/j.neulet.2010.03.060.

High frequency stimulation of the subthalamic nucleus evokes striatal dopamine release in a large animal model of human DBS neurosurgery

Young-Min Shon[a,c], **Kendall H. Lee**[a,b,*], **Stephan J. Goerss**[a], **In Yong Kim**[a], **Chris Kimble**[b], **Jamie J. Van Gompel**[a], **Kevin Bennet**[b], **Charles D. Blaha**[d], and **Su-Youne Chang**[a]

[a] Department of Neurological Surgery, Mayo Clinic, Rochester, MN 55905

[b] Division of Engineering, Mayo Clinic, Rochester, MN 55905

[c] Department of Neurology, The Catholic University of Korea, Seoul, Korea

[d] Department of Psychology, University of Memphis, Memphis, TN 38152

Abstract

Subthalamic nucleus deep brain stimulation (STN DBS) ameliorates motor symptoms of Parkinson's disease, but the precise mechanism is still unknown. Here, using a large animal (pig) model of human STN DBS neurosurgery, we utilized fast-scan cyclic voltammetry in combination with a carbon-fiber microelectrode (CFM) implanted into the striatum to monitor dopamine release evoked by electrical stimulation at a human DBS electrode (Medtronic 3389) that was stereotactically implanted into the STN using MRI and electrophysiological guidance. STN electrical stimulation elicited a stimulus time-locked increase in striatal dopamine release that was both stimulus intensity- and frequency-dependent. Intensity-dependent (1–7 V) increases in evoked dopamine release exhibited a sigmoidal pattern attaining a plateau between 5 to 7 V of stimulation, while frequency-dependent dopamine release exhibited a linear increase from 60 to 120 Hz and attained a plateau thereafter (120–240 Hz). Unlike previous rodent models of STN DBS, optimal dopamine release in the striatum of the pig was obtained with stimulation frequencies that fell well within the therapeutically effective frequency range of human DBS (120–180 Hz). These results highlight the critical importance of utilizing a large animal model that more closely represents implanted DBS electrode configurations and human neuroanatomy to study neurotransmission evoked by STN DBS. Taken together, these results support a dopamine neuronal activation hypothesis suggesting that STN DBS evokes striatal dopamine release by stimulation of nigrostriatal dopaminergic neurons.

Keywords

Deep brain stimulation; Dopamine release; Fast-scan cyclic voltammetry; Pig brain; Subthalamic nucleus; Parkinson's disease

Deep brain stimulation (DBS) of the subthalamic nucleus is an effective treatment for Parkinson's disease (PD) [2,23]. Because the therapeutic effects of DBS are similar to those

*Corresponding author: Kendall H. Lee, M.D., Ph.D., Department of Neurosurgery, Mayo Clinic, 200 First Street SW, Rochester, Minnesota 55905, Telephone: 507-284-2816; Fax: 507-284-5206; lee.kendall@mayo.edu.

of a lesion [4], DBS has been thought to silence STN neurons [3,24]. As an alternative to a silencing mechanism of STN DBS, we have hypothesized that electrical stimulation of the STN activates surviving nigrostriatal dopaminergic neurons to evoke significant dopamine release in the striatum that, in part, contributes to therapeutic effects in PD patients [18,21,22,6]. Support for a dopamine neuronal activation hypothesis of STN DBS comes from both basic research and clinical observations. For example, Zhao and colleagues [33] have shown in MPTP hemiparkinsonian rhesus monkeys that chronic (tested up to 10 months) STN DBS results in significant striatal dopamine elevation as measured by microdialysis that corresponded to improvements in symptoms. In PD patients, bilateral STN DBS decreases or eliminates the need for L-DOPA [26,25], it is *most* effective in PD patients who respond well to L-DOPA [8], and is contraindicated for those who do not respond to L-DOPA [15], suggesting that therapeutic DBS requires endogenous dopamine production in the striatum. DBS may even elicit dyskinesias that resemble those seen when excess L-DOPA is given [23] and impulsivity, a dopamine-related behavior [12]. Together these experimental and clinical observations suggest the hypothesis that STN DBS may evoke dopamine release from surviving nigrostriatal dopaminergic neurons projecting to the striatum to contribute to its therapeutic effects, as well as elicit unwanted side effects when combined with inappropriately high doses of L-DOPA.

In this regard, using electrochemical techniques, including fast scan cyclic voltammetry (FSCV), we have shown that high frequency stimulation (HFS) of the STN is capable of evoking striatal dopamine release in the intact rat [18,10]. In addition, we have also detected significant striatal dopamine release evoked by HFS of the STN in a well-recognized animal model of PD (dopamine nigrostriatal pathway lesions with 6-OHDA) [6]. Here, using a large animal (pig) model of human STN DBS neurosurgery, we applied FSCV in combination with a carbon-fiber microelectrode (CFM) stereotactically implanted into the striatum to monitor dopamine release evoked by a human DBS electrode unilaterally implanted into the STN. Several characteristics make the pig an excellent animal model to investigate STN DBS mechanisms in that it has face validity with human DBS surgery, and rivals that of DBS studies in non-human primate [32]. Adult pig brains (~160 g) are comparable in size to that of rhesus monkeys (~100 g) and baboons (~140 g), the volume of the pig STN (50±7 mm^3) is comparable to that of the rhesus monkey (34±6 mm^3) [14], and a pig brain atlas is available with significant similarities with human and non-human primates [11]. As such, we report here that the magnitude and temporal pattern of dopamine release evoked by STN electrical stimulation was both dependent upon stimulation frequency and intensity. Moreover, maximal dopamine release was obtained with stimulation parameters that are typically used with therapeutic DBS in PD patients.

The following experiments were performed in accordance with NIH guidelines (publication 86–23) and approved by the Mayo Clinic Institutional Animal Care and Use Committee. Four male pigs, weighing 26 – 30 kg, were initially sedated with Telazol (5 mg/kg i.m.) and xylazine (2 mg/kg i.m.), then intubated with endo-tracheal tube and ventilated with an artificial ventilator, then maintained with isoflurane (1%) for the remaining experimental procedure. In the prone position, the pig was placed in a MRI-compatible stereotactic head frame. A localizer box was then attached onto the head frame to create nine fiducials to enable localization of MR images in stereotactic space. For preoperative targeting of the STN, MRI was performed with a General Electric Signa 3.0 T system. The DICOM image data were then transferred to a stereotactic planning computer and the anterior commissure - posterior commissure line identified on the MR images. Using COMPASS navigational software, MRI data was then merged with a pig atlas [11] and stereotactic coordinates for the DBS electrode implantation trajectory defined (Fig. 1A and B).

Thereafter, in the operating room a large midline incision of the skin was made to expose the cranial landmarks of bregma and lambda. This was followed by a burr hole made on the skull in line with our trajectory coordinates. A tungsten extracellular microelectrode (0.5–1.0 MΩ), mounted onto a microdrive, was then lowered using the same trajectory for the DBS electrode obtained by the navigation software to identify the final dorsoventral coordinates of the STN. Following electrophysiologic confirmation of the STN coordinates, a Medtronic 3389 human DBS electrode was then implanted into the STN target. The pig was then returned to the MRI scanner for postoperative confirmation of the placement of the DBS electrode (Fig. 1D).

For FSCV measurements, the recording CFM was prepared by aspirating a single carbon-fiber into a glass capillary, pulling to a fine taper on a pipette puller (Model PE-2, Narashige, Tokyo, Japan), and sealing with nonconducting epoxy [9]. Borosilicate capillaries containing the carbon fiber were pulled by a laser-based micropipette puller (P-2000, Sutter Instrument Co., Navato, CA). FSCV recordings of STN DBS evoked striatal dopamine release were performed using the wireless instantaneous neurotransmitter concentration system (WINCS), as per our previous published procedures [7,31]. FSCV not only supports sub-sec measurements at a CFM, but additionally provides a chemical signature in the form of a background-subtracted voltammogram to identify the chemical origin of the signal [29]. FSCV parameters for dopamine measurements consisted of a −0.4 V rest potential, 1.5 V peak potential, 400 V/s scan rate, and 10 Hz scan application. In addition, to complete the circuit necessary for the FSCV a 14 mm burr hole was drilled on the contralateral side of the skull to allow the placement of an Ag/AgCl reference electrode. In a similar fashion to the DBS electrode, preoperative MRI data combined with the pig atlas [11] were used to define the trajectory and final stereotactic coordinates for implantation of the CFM electrode into the center of the head of the caudate (striatum; Fig. 1C).

Post-*in vivo* calibrations of the CFMs utilized in each experiment were performed using a flow injection analysis system [17,7]. Briefly, individual CFMs were placed in a flowing stream of solution in which various concentrations of dopamine (1 to 10 μM) were injected sequentially over a 10 s period using an electronic loop injector. The flowing solution consisted of buffered physiological saline (150 mM sodium chloride and 25 mM Hepes at a pH 7.4) pumped at a rate of 4 ml/min across the CFM, positioned in the center of the inflow tubing to a Plexiglas reservoir. An Ag/AgCl reference electrode was placed in the bottom of the flow cell reservoir immersed in the buffer solution. Injection of each dopamine concentration permitted the establishment of a dopamine calibration curve to assess the relationship between stimulation-evoked increases in dopamine oxidation current and dopamine extracellular concentration.

Using a hand held stimulator (Medtronic screener model 3628, Medtronic Inc., MN), a series of two-second duration biphasic, charge-balanced, voltage-isolated stimulations were delivered between lead 0 (most distal) and lead +1 of the Medtronic 3389 electrode (Medtronics Inc.) implanted in the STN. Electrical stimulation parameters included various intensities of stimulation at 3, 4, 5, and 7 volts with frequency held constant at 120 Hz, while frequency dependency was tested at 60, 90, 120, 150, 180, and 240 Hz with intensity held constant at 3 V, all at 0.5 msec pulse width. To maximize the reproducibility of each STN-evoked dopamine response, these stimulations were repeated on the basis of the number of pulses applied (a 5 min interstimulus interval was incrementally added to the total interstimulus period for every 120 pulses delivered).

Comparison of the pre- and post-operative MRI confirmed the accurate placement of the DBS electrodes within the STN of each of the four pigs tested (see Fig. 1A and D). As shown in Fig. 2A (Inset), STN DBS (2 s, 120Hz, 0.5 ms pulse width and 5V) results in a voltammogram, a plot of measured dopamine oxidation (ox.) and reduction (rd.) current versus the applied potential, that provides a signature to identify the recorded chemical. For dopamine, oxidation

during the positive scan and reduction of the electroformed dopamine ortho-quinone (DOQ) back to dopamine during the negative scan results in two distinct current peaks. These peaks are clearly observed when voltammograms recorded in the striatum are plotted sequentially, with oxidation and reduction current magnitude designated by a pseudo-color plot (Fig. 2B; x-axis: time [sec], y-axis: applied scanning potential [V], z-axis: ox. and rd. current [nA]) or with only oxidation current magnitude plotted with respect to time (Fig. 2A: x-axis: time [sec], y-axis: current [nA]) during and after electrical stimulation of the STN [5]. Changes in the amplitude of the dopamine oxidation peak recorded by FSCV thus provide a quantitative concentration measurement of the temporal effects of electrical stimulation of the STN on dopamine release.

As shown in Fig. 3A for one representative pig, while holding the STN stimulation frequency constant (120 Hz), increasing voltage intensity from 3 to 7 V resulted in a progressive increase in the magnitude of striatal dopamine release and duration of recovery to pre-stimulation baseline levels. A plot of the maximal increases in dopamine release observed at each of the stimulation intensities revealed clear sigmoidal-like intensity-dependent responses for three of the pigs tested (Fig. 3B). In contrast, with stimulation intensity held constant (3 V), increasing stimulation frequency from 60 to 240 Hz resulted in a linear increase in the peak magnitude of striatal dopamine release within 60 to 120 Hz and a plateau at and above 120 Hz (Fig. 3C). The duration of post-stimulation recovery to pre-stimulation baseline levels for 60 to 240 Hz ranged from 4 to 10 sec (data not shown).

In summary, in the large animal (pig) model of DBS surgery, we demonstrate that electrical stimulation of the STN elicited a stimulation time-locked increase in striatal dopamine release that was dependent on both stimulation intensity and frequency. In the case of stimulation intensity, the increase in evoked dopamine release exhibited a sigmoidal pattern in all three pigs tested, attaining a plateau at around 7 V of stimulation with a fixed frequency of 120 Hz. However, the maximal concentration in extracellular dopamine attained by these applied stimulus intensities exhibited a relatively high degree of variance between animals (1–4 μM). The variance observed in intensity evoked dopamine responses between animals are not unexpected given the heterogeneity of dopaminergic innervation of the striatum where the recording electrode was located [28] and the precise location of the stimulating electrode within the STN. In contrast to the stimulation intensity dependency, over a range of stimulation frequencies (60 to 240 Hz) and fixed intensity (3 V), striatal dopamine release exhibited a linear increase up to 120 Hz and thereafter attained a plateau.

Anatomically, STN glutamatergic neurons are known to project to dendrites of SNc dopaminergic cells [1,16], suggesting that STN stimulation evoked increases in dopamine release in the ipsilateral striatum likely results from STN glutamatergic activation of SNc dopaminergic neurons [18,30]. Indeed, we have shown previously in the rat that similar STN electrical stimulation resulted in excitatory postsynaptic potentials in SNc dopaminergic neurons *in vitro* [19,20] and increases in striatal dopamine release *in vivo* [18]. Alternatively, given the placement of the DBS electrodes, it is also conceivable that the evoked dopamine release may be due to direct stimulation of dopaminergic fibers of passage which are known to course within the medial forebrain bundle lying immediately dorsal to the STN [18].

Optimal clinical results in PD patients have been routinely obtained using stimulation intensities of 2–5 V and frequencies of 120–180 Hz delivered in the STN [13,27]. Thus, it is important to note that maximal dopamine release observed here in striatum of the pig were obtained only with STN stimulation parameters that fell within the range of human therapeutic DBS parameters. In this regard, we have shown in the rat that striatal dopamine release could be evoked using low to high frequency stimulation (5–300 Hz) of the STN [18]. However, in contrast to the present data, in the rat a peak dopamine release response was seen at 50 Hz with

the response falling off at 75 Hz and greater. As such, these present findings highlight the critical importance of examining neurochemical mechanisms of STN DBS in a large animal model (pig) that more closely represents human neuroanatomy and DBS electrode configuration. Taken together, these results support further investigations of the dopamine neuronal activation hypothesis [18,21,22,6] utilizing a versatile and economically affordable animal model of human STN DBS.

Acknowledgments

Drs. Youg-Min Shon and Kendall H. Lee contributed equally to this work. We wish to thank the contribution of the engineers of Division of Engineering of Mayo Clinic, April E. Horne, David M. Johnson, Kenneth R. Kressin, Justin C. Robinson, Sidney V. Whitlock and Bruce A. Winter for their invaluable efforts in the realization of the WINCS device and software. This work was supported by NIH (K08 NS 52232 award) and Mayo Foundation (2008–2010 Research Early Career Development Award for Clinician Scientists) to KHL.

References

1. Albin RL, Young AB, Penney JB. The functional anatomy of basal ganglia disorders. Trends Neurosci 1989;12:366–375. [PubMed: 2479133]
2. Benabid AL, Koudsie A, Benazzouz A, Fraix V, Ashraf A, Le Bas JF, Chabardes S, Pollak P. Subthalamic stimulation for Parkinson's disease. Arch Med Res 2000;31:282–289. [PubMed: 11036179]
3. Benazzouz A, Piallat B, Pollak P, Benabid AL. Responses of substantia nigra pars reticulata and globus pallidus complex to high frequency stimulation of the subthalamic nucleus in rats: electrophysiological data. Neurosci Lett 1995;189:77–80. [PubMed: 7609923]
4. Bergman H, Wichmann T, DeLong MR. Reversal of experimental parkinsonism by lesions of the subthalamic nucleus. Science 1990;249:1436–1438. [PubMed: 2402638]
5. Bergstrom BP, Garris PA. Utility of a tripolar stimulating electrode for eliciting dopamine release in the rat striatum. J Neurosci Methods 1999;87:201–208. [PubMed: 11230817]
6. Blaha, CD.; Lester, DB.; Ramsson, ES.; Lee, KH.; Garris, PA. Striatal dopamine release evoked by subthalamic stimulation in intact and 6-OHDA-lesioned rats: Relevance to deep brain stimulation in Parkinson's Disease. In: Phillips, PEM.; Sandberg, SG.; Ahn, S.; Phillips, AG., editors. Monitoring Molecules in Neuroscience. University of British Columbia; Vancouver, BC: 2008. p. 395-397.
7. Bledsoe J, Kimble C, Covey D, Blaha CD, Agnesi F, Mohseni P, Whitlock S, Johnson D, Horne A, Bennet K, Lee K, Garris P. Development of wireless instantaneous neurotransmitter concentration system (WINCS) for intraoperative neurochemical monitoring using fast-scan cyclic voltammetry. J Neurosurg 2009;111:712–723. [PubMed: 19425890]
8. Breit S, Schulz JB, Benabid AL. Deep brain stimulation. Cell Tissue Res 2004;318:275–288. [PubMed: 15322914]
9. Cahill PS, Walker QD, Finnegan JM, Mickelson GE, Travis ER, Wightman RM. Microelectrodes for the measurement of catecholamines in biological systems. Analyt Chem 1996;68:3180–3186. [PubMed: 8797378]
10. Covey, DP.; Ramsson, ES.; Heidenreich, BA.; Blaha, CD.; Lee, KH.; Garris, PA. Monitoring subthalamic nucleus-evoked dopamine release in the striatum using fast-scan cyclic voltammetry in vivo. In: Phillips, PEM.; Sandberg, SG.; Ahn, S.; Phillips, AG., editors. Monitoring Molecules in Neuroscience. University of British Columbia; Vancouver, BC: 2008. p. 398-400.
11. Felix B, Leger ME, Albe-Fessard D, Marcilloux JC, Rampin O, Laplace JP. Stereotaxic atlas of the pig brain. Brain Res Bull 1999;49:1–137. [PubMed: 10466025]
12. Frank MJ, Samanta J, Moustafa AA, Sherman SJ. Hold your horses: impulsivity, deep brain stimulation, and medication in parkinsonism. Science 2007;318:1309–1312. [PubMed: 17962524]
13. Garcia L, D'Alessandro G, Bioulac B, Hammond C. High-frequency stimulation in Parkinson's disease: more or less? Trends Neurosci 2005;28:209–216. [PubMed: 15808356]
14. Hardman CD, Henderson JM, Finkelstein DI, Horne MK, Paxinos G, Halliday GM. Comparison of the basal ganglia in rats, marmosets, macaques, baboons, and humans: volume and neuronal number

for the output, internal relay, and striatal modulating nuclei. J Comp Neurol 2002;445:238–255. [PubMed: 11920704]

15. Kern DS, Kumar R. Deep brain stimulation. Neurologist 2007;13:237–252. [PubMed: 17848864]
16. Kita H, Kitai ST. Efferent projections of the subthalamic nucleus in the rat: light and electron microscopic analysis with the PHA-L method. J Comp Neurol 1987;260:435–452. [PubMed: 2439552]
17. Kristensen EW, Wilson RM, Wightman RM. Dispersion in flow injection analysis measured with microvoltammetric electrodes. Analyt Chem 1986;58:986–988.
18. Lee KH, Blaha CD, Harris BT, Cooper S, Hitti FL, Leiter JC, Roberts DW, Kim U. Dopamine efflux in the rat striatum evoked by electrical stimulation of the subthalamic nucleus: potential mechanism of action in Parkinson's disease. Eur J Neurosci 2006;23:1005–1014. [PubMed: 16519665]
19. Lee KH, Roberts DW, Kim U. Effect of high-frequency stimulation of the subthalamic nucleus on subthalamic neurons: an intracellular study. Stereotactic Funct Neurosurg 2003;80:32–36.
20. Lee KH, Chang SY, Roberts DW, Kim U. Neurotransmitter release from high-frequency stimulation of the subthalamic nucleus. J Neurosurg 2004;101:511–517. [PubMed: 15352610]
21. Lee, KH.; Blaha, CD.; Bledsoe, JM. Mechanisms of action of deep brain stimulation: A review. In: Krames, E.; Hunter Peckham, P.; Rezai, A., editors. A Textbook of Neuromodulation. Elsevier; Amsterdam: 2008. p. 54-79.
22. Lee KH, Blaha CD, Garris PA, Mohseni P, Horne AE, Bennet KE, Agnesi F, Bledsoe JM, Lester DB, Kimble C, Min HK, Kim YB, Cho ZH. Evolution of deep brain stimulation: human electrometer and smart devices supporting the next generation of therapy. Neuromodulation 2009;12:85–103.
23. Limousin P, Krack P, Pollak P, Benazzouz A, Ardouin C, Hoffmann D, Benabid AL. Electrical stimulation of the subthalamic nucleus in advanced Parkinson's disease. N Engl J Med 1998;339:1105–1111. [PubMed: 9770557]
24. Lozano AM, Dostrovsky J, Chen R, Ashby P. Deep brain stimulation for Parkinson's disease: disrupting the disruption. Lancet Neurol 2002;1:225–231. [PubMed: 12849455]
25. Molinuevo JL, Valldeoriola F, Tolosa E, Rumia J, Valls-Sole J, Roldan H, Ferrer E. Levodopa withdrawal after bilateral subthalamic nucleus stimulation in advanced Parkinson disease. Arch Neurol 2000;57:983–988. [PubMed: 10891980]
26. Moro E, Scerrati M, Romito LM, Roselli R, Tonali P, Albanese A. Chronic subthalamic nucleus stimulation reduces medication requirements in Parkinson's disease. Neurology 1999;53:85–90. [PubMed: 10408541]
27. Moro E, Esselink RJ, Xie J, Hommel M, Benabid AL, Pollak P. The impact on Parkinson's disease of electrical parameter settings in STN stimulation. Neurology 2002;59:706–713. [PubMed: 12221161]
28. Nomoto M, Kaseda S, Iwata S, Shimizu T, Fukuda T, Nakagawa S. The metabolic rate and vulnerability of dopaminergic neurons, and adenosine dynamics in the cerebral cortex, nucleus accumbens, caudate nucleus, and putamen of the common marmoset. J Neurol 2000;247:16–22.
29. Robinson DL, Venton BJ, Heien ML, Wightman RM. Detecting subsecond dopamine release with fast-scan cyclic voltammetry *in vivo*. Clin Chem 2003;49:1763–1773. [PubMed: 14500617]
30. Shimo Y, Wichmann T. Neuronal activity in the subthalamic nucleus modulates the release of dopamine in the monkey striatum. Eur J Neurosci 2009;29:104–113. [PubMed: 19087163]
31. Shon YM, Chang S-Y, Tye S, Kimble C, Bennet K, Blaha CD, Lee KH. Co-monitoring of adenosine and dopamine using the Wireless Instantaneous Neurotransmitter Concentration System (WINCS): proof of principle. J Neurosurg. 2009 in press. E-Pub Ahead of Print.
32. Wakeman DR, Crain AM, Snyder EY. Large animal models are critical for rationally advancing regenerative therapies. Regen Med 2006;1:405–413. [PubMed: 17465832]
33. Zhao X, Caob Y, Liuc H, Lid F, Youd B, Zhou X. Long term high frequency stimulation of STN increases dopamine in the corpus striatum of hemiparkinsonian rhesus monkey. Brain Res 2009;1286:230–238. [PubMed: 19563788]

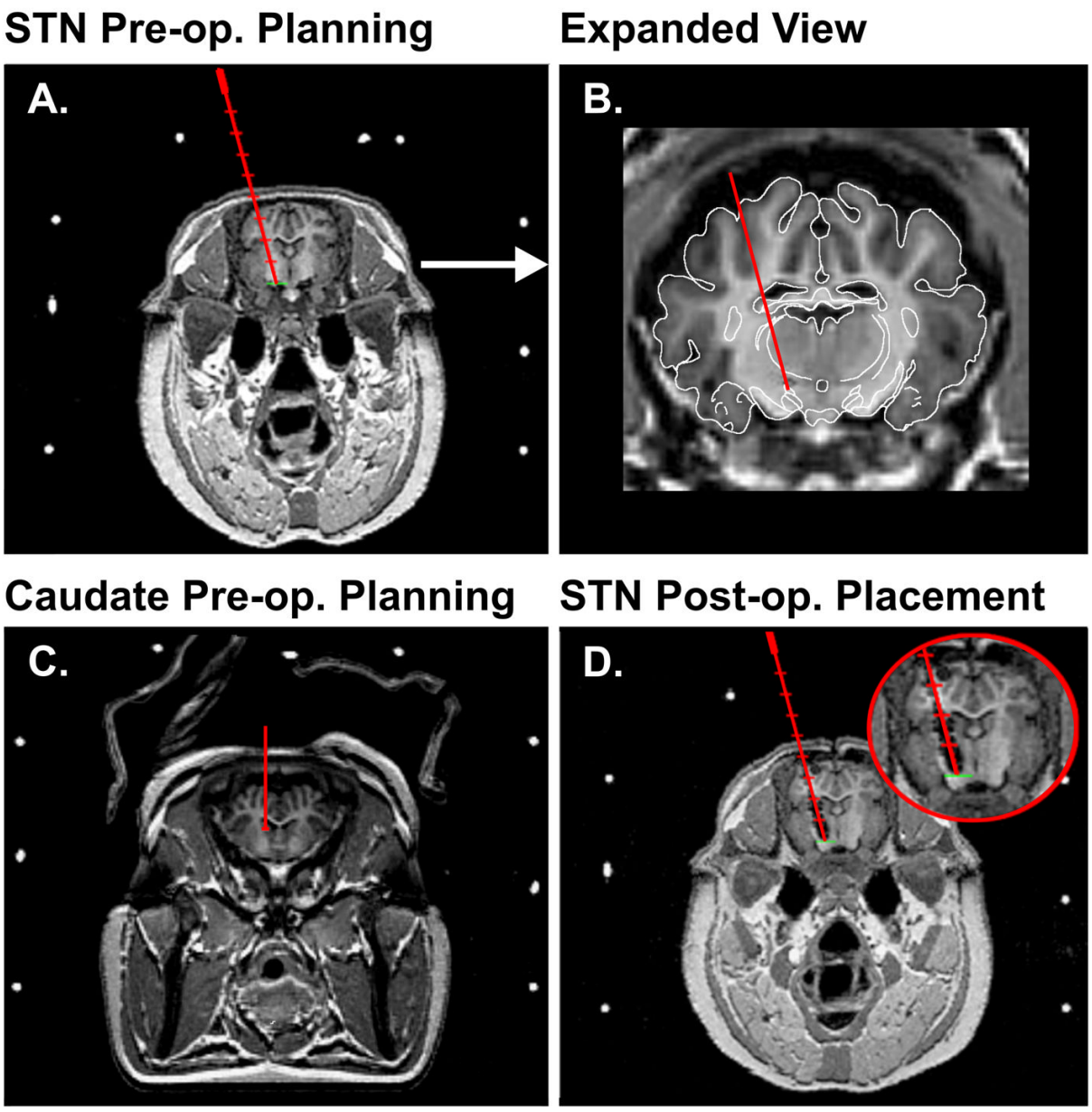

Fig. 1.

(A.) A representative coronal MRI and corresponding fiducials (white circles) on the MRI-compatible head frame for pre-operative planning and calculation of the trajectory coordinates (red line) for implantation of a DBS electrode in the STN of the pig. (B.) Expanded view of the pre-operatively planned trajectory for implantation of a DBS electrode in the STN. (C.) A representative coronal MRI for pre-operative planning and calculation of the trajectory coordinates (red line) for implantation of a carbon-fiber recording electrode in the caudate of the pig. (D.) A coronal MRI showing the post-operative confirmation of the DBS electrode placement in the STN of the pig shown in (A).

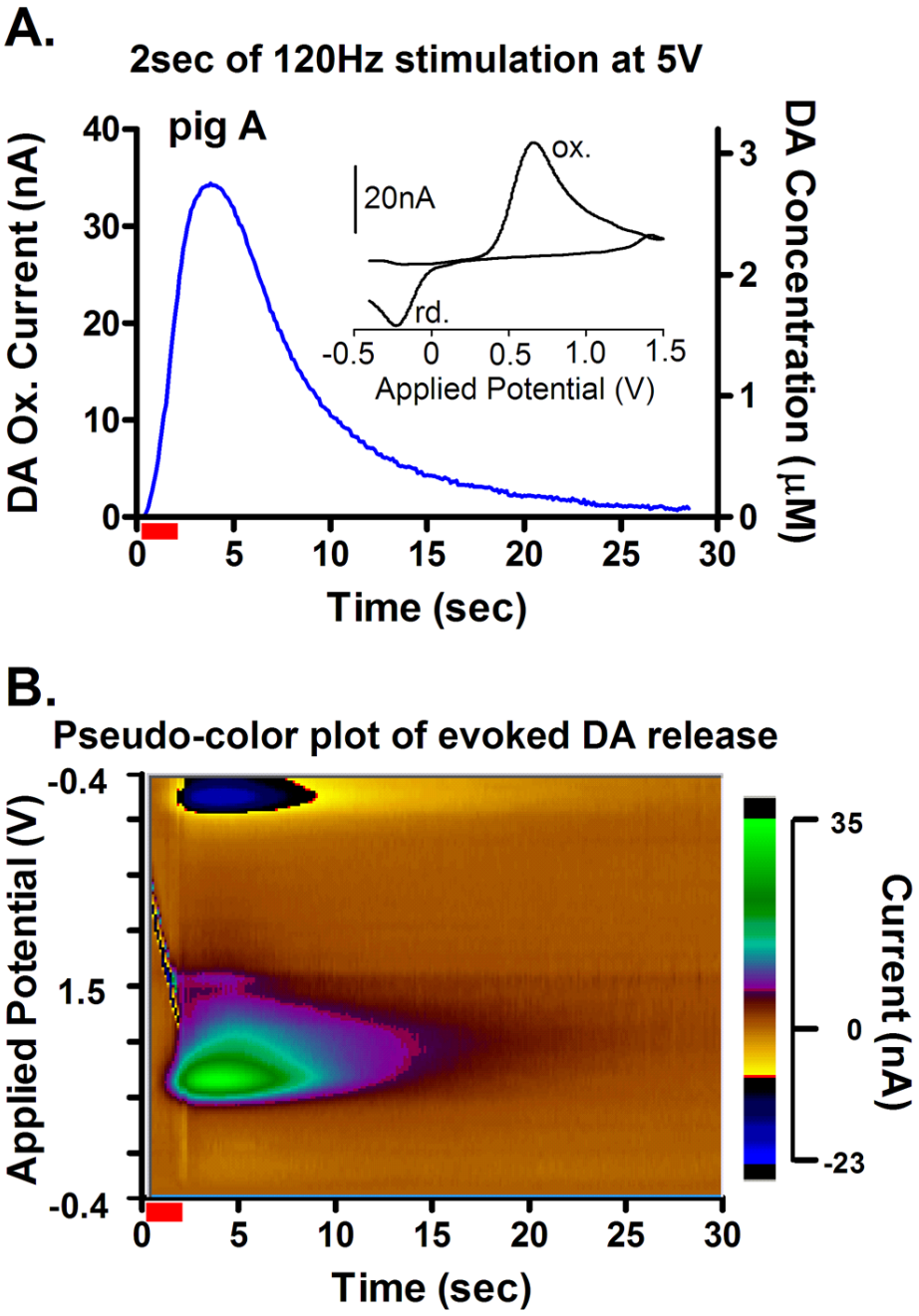

Fig. 2.

(A.) *In vivo* characteristics of dopamine release recorded in pig "A" striatum during 2-sec (red bar) STN stimulation with 5 V at 120 Hz. (Inset) A cyclic voltammogram recorded at the peak of the evoked increase in dopamine release characteristic of dopamine oxidation (ox.) and reduction (rd.) of the electroformed dopamine ortho-quinone (DOQ) back to dopamine. (B.) Pseudo-color plot obtained during (red bar) and after 2-sec STN stimulation with 5 V at 120Hz.

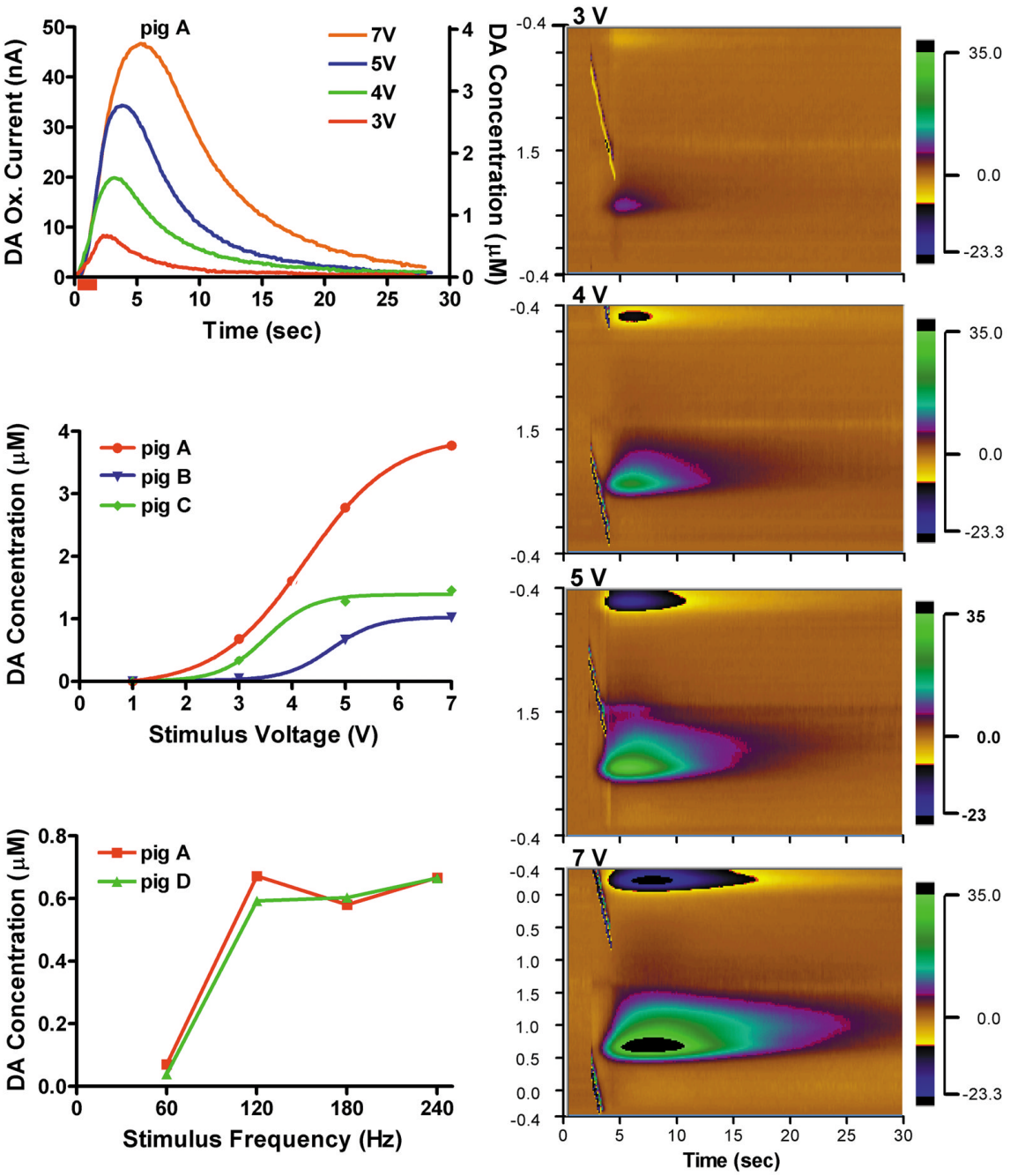

Fig. 3.

(A.) *In vivo* characteristics of dopamine release recorded in pig "A" striatum during 2-sec (red bar) STN stimulation with 3 to 7 V at 120 Hz. Right panel shows representative pseudo-color plots obtained immediately prior to, during (red bars), and after 2-sec STN stimulation with 3, 4, 5, and 7 V at 120Hz. (B.) STN stimulation intensity-dependent increases in dopamine release from 3 pigs ("A", "B", and "C"). Each curve describes the best non-linear fit (square, $r^2 = 0.99$). (C.) STN stimulation frequency-dependent (60 to 240 Hz at 3 V) increases in dopamine release from pig "A" and pig "D".